

Durability Study of a Polymeric Composite Material for Structural Applications

M. S. AL-HAIK¹ and H. GARMESTANI^{1,2*}

¹*Department of Mechanical Engineering, FAMU-FSU College of Engineering
Florida A&M University-Florida State University, Tallahassee, FL 32316*

²*Center for Materials Research and Technology (MARTECH)
Florida State University
Tallahassee, Florida, 32316*

An experimental study was carried out to investigate the mechanical behavior of a structural carbon based composite for infrastructure industry. Creep and load relaxation experiments were conducted to investigate the rate sensitivity behavior for a temperature range of 20–60°C. The results show that the mechanical properties were degraded under elevated temperature conditions. A threshold stress was measured, at any given temperature, below which no observable strain rate is detected. Results show that load relaxation experiment can be used as an effective tool to study durability and long-time creep behavior. The load relaxation test methodology for the prediction of model parameters was found to be more time and cost efficient than traditional long-time creep tests.

1. INTRODUCTION

Structural composites possessing superior strength/weight and modulus/weight characteristics including high performance fiber (glass, carbon, aramid and hybrid) reinforced composites with polymer matrices are being considered as alternative materials for structural applications (1). The relative ease of manufacturing lightweight components and the wide range of physical properties and several other outstanding properties make polymer matrix composites (PMCs) very attractive for industrial applications (2–4).

For industrial applications, the composite is subjected to a complicated loading history requiring changes in several processes, which occur simultaneously—strength and modulus degradation, stress level relaxation, and creep. Each of these processes has its own load, time, and temperature dependence. Therefore, all effects must be accounted for in the long-term durability investigation of the composite. It is clear that to predict the mechanical degradation in such loading conditions, a constitutive model is needed that can capture the largest strain rate behavior of the material at higher temperatures and severe environmental conditions.

Over the last two decades, durability prediction of polymer matrix composites has become the keystone in structural design. Strain rate sensitivity together with the high strength and durability determines the reliability of the composite structural parts. The reliability for long-term structural applications under severe conditions of temperature is an important factor for composite usage. Imperatively, any discussion of the sustained use of a structural material must address the performance of PMCs under loads applied for extended periods of time (5, 1).

The current trend toward the use of PMCs in infrastructure applications demands durability under different loading conditions. This requires better understanding of the composite behavior under service conditions. While fibers are the main source of the tremendous strength and stiffness properties of the PMCs, the matrix-related properties are of primary importance for all types of loading (tensile, creep, relaxation) in long = term applications. When a polymeric matrix is heated to a temperature below its glass transition temperature, T_g° , the material is no longer in a stable thermodynamic state. This results in a change in mechanical properties such as yield stress, creep resistance, toughness and viscosity and is known as physical aging (6–13).

Constitutive modeling of PMCs to cover a wide range of strain rate and strain range presents a distinct challenge. Although progress had been made in

*Corresponding author. E-mail: garm@magnet.fsu.edu.

constructing models for small strain and temperature regimes, (6, 14, 15), much less progress had been made for predicting the durability of PMCs for long-term exposure to high temperatures. PMCs can become brittle, viscoelastic or viscoplastic depending on the loading conditions to which they are exposed. The major hindrance in modeling the PMC behavior is that mechanisms of deformation in polymers seem to be more complicated than those in metals. Hence, classical constitutive models and concepts for metals are not directly applicable to modeling polymers and polymer composites. Analytical models were proposed to predict the strain rate behavior of PMCs. A deterministic approach was proposed by Gates (16), who provided test methods and an elastic/viscoplastic constitutive model that accounts for some aspects of rate dependent tension and compression loading behavior of PMC materials throughout the temperature range. These tests included stress relaxation and creep. However, these models have been applied to relaxation results with very short time duration and as a result the simulations covered a very small strain rate regime. Similar approaches based on the viscoplastic nature of PMCs are discussed thoroughly by Drozdov, (17), Bardenhagen (18) and Fish (19).

The industrial applications of PMCs underline the necessity for long-term performance of those materials. In order to realize much of the potential of PMCs, tools to accelerate testing and predicting long-term performance were generated by several investigators. The long-term exposure of PMCs to service environmental conditions degrades original properties. One powerful method to extract long-term response from accelerated tests of PMCs is time-temperature superposition (21). Information on long-term deformation and strength is normally obtained via these accelerated tests by extrapolation of the short-term test data, obtained under accelerated testing conditions. Such tests can include experiments at higher temperatures,

stress and humidity. A unified model is usually necessary to simulate the service conditions (22, 23).

If the material is stable, i.e. no structural change during deformation, and satisfies a viscoplastic law in simple tension, we may use stress relaxation tests, which can be utilized to obtain, in considerably shorter time, the strain rates corresponding to the same stress in creep tests. This data can make it possible to extract long-term behavior in creep or other complex loading behavior from relaxation tests for a considerably shorter time.

2. MECHANICAL TESTING THEORY

During a tensile test, a loading rate is applied to the actuator of a servo-hydraulic machine or the rotation of a DC motor in a screw-driven machine. The load is distributed uniformly in the mechanical testing chain that includes the specimen (deforming elastically and inelastically), the grip system and the load cell (deforming elastically), as shown schematically in Fig. 1.

Stress Relaxation Test

Load relaxation may occur naturally in some important applications. Consider the classical case of a pre-stressed bolt where some internal stress is left by tightening beyond the elastic limit of the material. In cases where the metallic bolt is viscoplastic (or in extreme conditions of high temperatures), such stresses may relax in the same manner as in a load relaxation experiment. Of more relevance is the ability to predict how stress will relax in structures in which the length of the component is kept constant. For a more relevant example, consider a concrete column that is reinforced with a composite. An initial tensile stress to the composite tendons results in a compressive stress in the aggregate. If the tensile stress in the composite relaxes with time, the pre-stressed concrete will lose its unique properties.

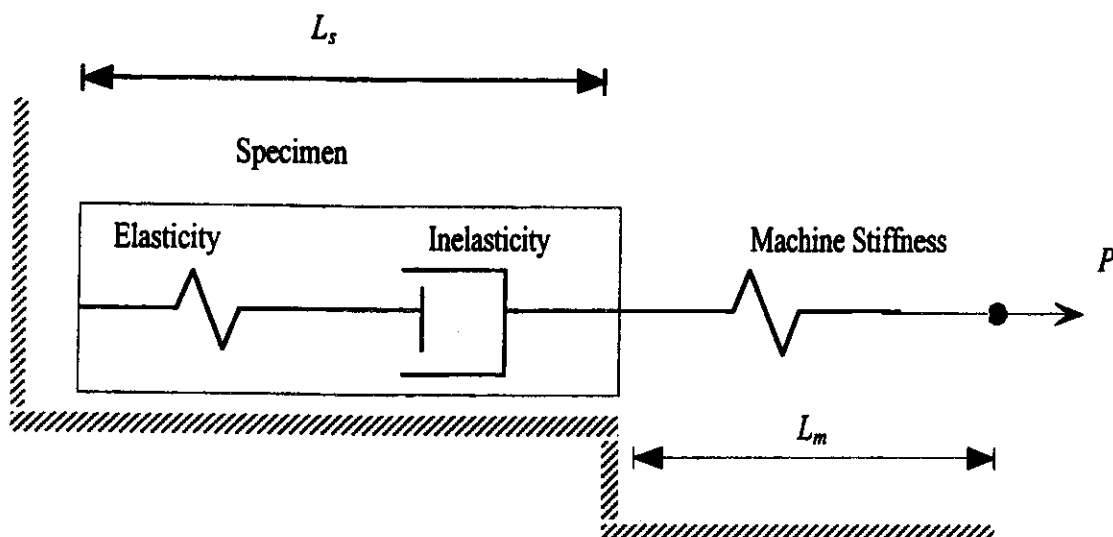


Fig. 1. Spring-dashpot analog for a mechanical testing system.

Stress relaxation can be defined as the decrease in stress in a solid under a constant strain, or extension at a constant temperature. This decrease in stress, in the case of a one-phase polycrystalline material, is the result of dislocations moving, overcoming localized barriers (24). ASTM standard E328 describes a number of experimental steps designed to perform stress relaxation correctly. One of the major issues in using the relaxation data is the contribution of machine compliance. In both screw-driven and servohydraulic machines, the machine compliance may be large and depend upon the major components used in the design. It has been found (24) that screw-driven machines have a definite stiffness, which relaxes during the test when the machine and specimen stiffnesses are of the same order of magnitude. In the following, it will be shown that the machine compliance for both machines can be measured and incorporated in the calculations. Servohydraulic machines operating under strain-control mode provide infinite stiffness, hence eliminating machine relaxation (25). One can use the spring-dashpot analog to describe the response of the machine-specimen system to deformation. The elastic (time-independent) portion of deformation is represented by the spring, and the inelastic (time-dependent) portion is represented by the dashpots, as seen in Fig. 1. During load relaxation, the total change in length for both the machine and the specimen becomes zero:

$$[\Delta L_e + \Delta L_i]_s + [\Delta L_e]_m = 0 \quad (1)$$

where $(\Delta L_e + \Delta L_i)_s$ is the elastic and inelastic change in the specimen length, and ΔL_m is the change in the extension resulting from the load frame.

The stiffness of the machine is represented as

$$K_m = \frac{dP}{dL_{em}} \quad (2)$$

where P is the total load and L_{em} is the elastic elongation of the machine. Taking the time derivative of Eq 1 and using Eq 2. Hence,

$$\dot{L}_e + \dot{L}_i + \frac{\dot{P}}{K_m} = 0 \quad (3)$$

Dividing Eq 3 by the length of the specimen at the onset of relaxation, we obtain the strain rates as

$$\dot{\epsilon}_e + \dot{\epsilon}_i = -\frac{\dot{P}}{K_m L_0} = -\frac{A_0}{K_m L_0} \dot{\sigma} \quad (4)$$

where $\dot{\epsilon}_e$ and $\dot{\epsilon}_i$ are elastic and inelastic strain rate in the specimen respectively, and $\dot{\sigma}$ is the stress rate.

The elastic strain in the specimen is related to the stress by Young's modulus and

$$\epsilon_e = \frac{\sigma}{E}$$

Hence, the specimen inelastic strain during the relaxation test is given by

$$\epsilon_i = -\left(\frac{A_0}{K_m L_0} + \frac{1}{E}\right)\sigma \quad (5)$$

where σ is the nominal stress, ϵ_i is the inelastic strain, L_0 is the initial gauge length, A_0 is the original cross-sectional area, and E is the Young's modulus of the sample.

From the above equations, it is clear that the machine stiffness K_m can influence the results if the strain is not measured directly from the specimen. Eq 5 can be rewritten as

$$\epsilon_i = \frac{\sigma}{E_A} \quad (6)$$

where E_A is defined as an apparent elastic modulus in the elastic region.

$$\frac{1}{E_A} = \frac{1}{E} + \frac{A_0}{L_0 K_m} \quad (7)$$

The stress relaxation test provides σ' as a function of stress (slope of the stress versus time curve at various stress levels). From this data, inelastic strain rate of the specimen can be calculated as a function of stress, prior strain history, and a number of state variables, X ,

$$\epsilon_i = f(\sigma, \epsilon, X) \quad (8)$$

Together with Eq 7, the relaxation time is shown to be inversely proportional to the apparent modulus

$$\Delta t = -\frac{1}{E_A} \int_{\sigma_i}^{\sigma_f} \frac{d\sigma}{f(\sigma, \epsilon, X)} \quad (9)$$

where σ_i and σ_f are the initial and final stresses respectively. Equation 9 shows that in order to reduce the time of relaxation, it is important to minimize the apparent modulus (26, 27).

Extrapolation of short-term test results for very long time periods is a fundamental problem in the analysis of structures whose lifetime is measured in years or decades. A reasonable duration for commonly performed tests is in the order of an hour, a day, even a month, but not longer. It has been suggested that the relaxation data may be used to extrapolate the creep and inelastic behavior at longer times (16, 25, 26). Lemaitre (28) showed that the time necessary for attaining a state characterized by particular values of the stress, plastic strain, and plastic strain rate is of the order 5–50 times shorter for relaxation than for creep. Grzywnski (29) and Findley (30) cited similar conclusions.

Creep Test

The creep test is usually performed by loading a specimen to a specific load and the load is then maintained at a constant value and the strain is recorded. During creep experiments, the load remains constant

$$\dot{P} = 0 \quad (10)$$

since the total strain can be decomposed into elastic and inelastic components;

$$\epsilon = \epsilon_e + \epsilon_i \quad (11)$$

the strain rate $\dot{\epsilon}$ is found by differentiating Eq 11 and noting that ϵ_e is a constant

$$\dot{\epsilon} = \dot{\epsilon}_t \quad (12)$$

Although creep and relaxation are different kinds of testing, they are related in the sense that they both measure the strain rate sensitivity of materials under a specific load (for creep) and total strain (for relaxation). The difference is the fact that a much larger strain (deformation) is involved during creep than during load relaxation. The extent of the deformation for the load relaxation is determined from machine compliance. On the other hand, if the material satisfies a viscoplastic law in simple tension, of the form,

$$\sigma = f(\epsilon_p, \dot{\epsilon}_p) \quad (13)$$

then there is an experimental method that can be used to obtain, by relaxation, in considerably shorter times, the strain rates that correspond to those in creep tests. This makes it possible to construct

long-term creep curves from short relaxation tests (28). The methodology is illustrated in Fig. 2. To find the strain corresponding to a constant stress σ^* at temperature T^* , we consider multiple relaxation tests performed with each relaxation reaching a limiting stress, σ^* . At every point of the relaxation curves $\sigma(t)$ where $\sigma = \sigma^*$ the material state is given by:

$$\begin{aligned} \sigma &= \sigma^* \\ \epsilon_p &= \epsilon - \frac{\sigma^*}{E} \\ \dot{\epsilon}_p &= -\dot{\sigma}(\sigma^*)/E \end{aligned} \quad (14)$$

The constitutive equations above link σ , ϵ_p , $\dot{\epsilon}_p$ for any loading history and so the values should also be representative of a creep test at $\sigma = \sigma^*$. This is with the assumption that the strain history (during creep) does not vary σ^* significantly! We may therefore trace the trajectory of the creep test by plotting a graph $(\epsilon_p, \dot{\epsilon}_p)$ and by integrating the function whose curve is that

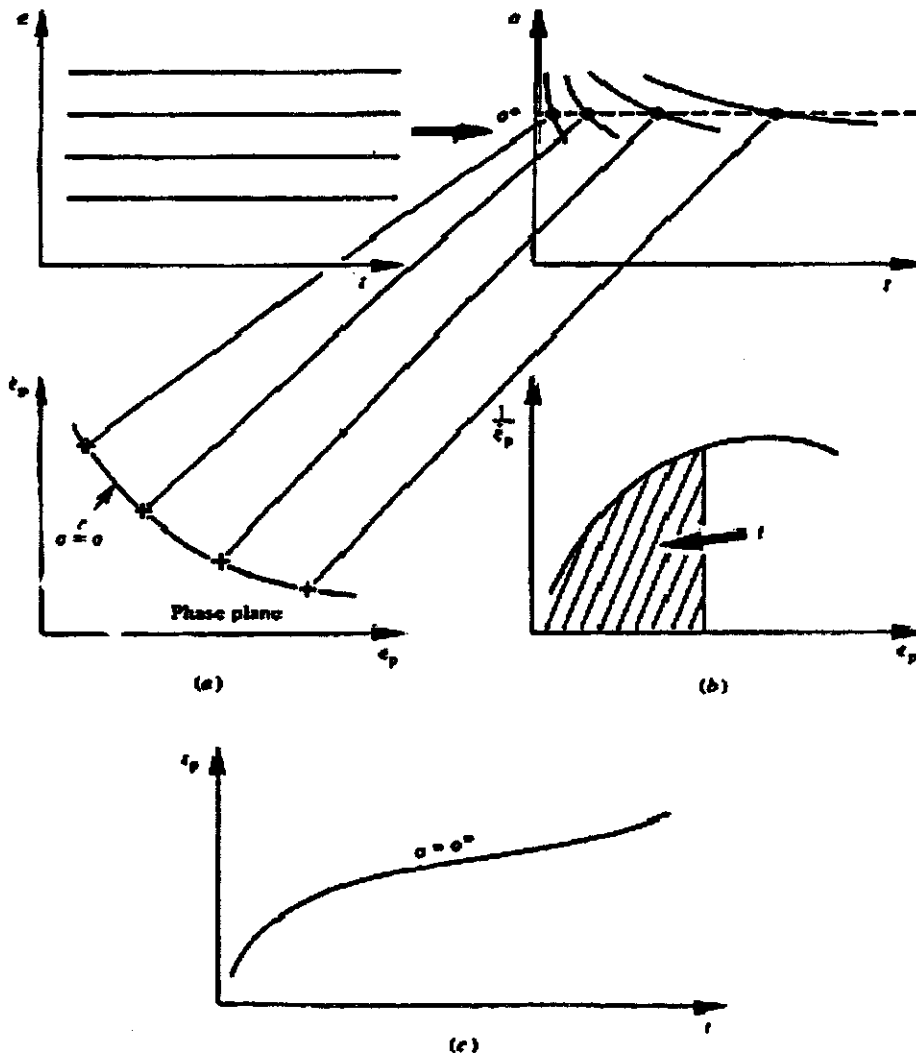


Fig. 2. Schematic illustration of the relaxation-creep method: (a) relaxation tests, (b) Creep trajectory, (c) Creep curve, Lemaitre (29).

which passes through these points, denoting this function by $g(\epsilon_p) = \dot{\epsilon}_p$, we obtain the creep curve $\epsilon_p(t)$ where creep time can be calculated from

$$t = \int_{\epsilon_{p0}}^{\epsilon_p} \frac{1}{g(\epsilon_p)} d\epsilon_p \quad (15)$$

So the inelastic strain rate in a relaxation test can be used to find out the plastic strain at a creep test, as illustrated from the formulation above, given by Lemarite, (28). Similar approaches to link the strain rate of relaxation and creep tests were performed by Gates (9) and Grzywinski (29).

Creep and load relaxation experiments are related in the sense that they both measure the strain rate sensitivity of materials under a specific load. If the internal material structure does not change during these tests, there exists one unique strain rate for each stress level. The total strain during a load relaxation test is less than 0.2% and as a result it can be assumed that the internal structure remains constant. Such a condition may not be valid for a creep test since a much larger strain is consumed. The other factor that may influence the results is the transients due to anelasticity. Anelastic strain is defined as the time-dependent component of the inelastic strain that is recoverable. Other factors influencing the results are the machine response time, temperature stability, and sampling rate for data acquisition. A crucial parameter in validating the flow stress response to changes in strain-rate is the machine response time. The environmental temperature stability and isolation from vibration (which may become substantial for hydraulic type testing machines) are among other important experimental variables. The flow stress of the material is directly related to the temperature of the material and must remain constant to correctly evaluate the material response. The temperature stability is important for both creep and relaxation experiments. For load relaxation experiments, an accurate measurement of lower strain rate (below 10^{-6}) requires a temperature stability of 0.2°C .

3. MATERIALS

A structural carbon reinforced composite material is used for the investigation of viscoplastic-viscoelastic properties. The materials were provided by the Florida Department of Transportation.

I-Fibers: Thornel T-300 12K was used as the carbon fiber material in this study. This fiber is a continuous length, high strength, and high modulus fiber consisting of 12,000 filaments in a one-ply construction. The diameter of each fiber is 7 microns. The fiber surface has been treated to increase the interlaminar shear strength in a resin matrix composite. The tensile strength is 3.65 GPa, and the elastic modulus is 231 GPa, Table 1.

II-Matrix: Thixotropic epoxy was used as the matrix. This epoxy is manufactured by PTM & W industries, Inc. under the brand name PR2032. It is a medium

Table 1. Typical Properties of Thornel Carbon Fiber T-300 12 K.

Property	Value
Tensile Strength	3.65 GPa
Tensile Modulus	231 GPa
Filament Diameter	7 mm
Density	1.76 Mg/m ³
Elongation at Failure	1.4%
Surface Area	0.45 m ² /g

viscosity, unfilled, light amber laminating resin that is designed for structural production applications. This resin laminates very easily, and wets out fiberglass, carbon, and aramid fibers readily. Used with PH3660 hardener, this system cures at a minimum temperature of 72°F and should be cured at least 24 hours before use. Typical properties of this epoxy are listed in Table 2.

4. FABRICATION AND TESTING OF COMPOSITE SAMPLES

The composites were fabricated in a layer-by-layer manual technique. In conditions where the composite is used for repair of columns and damaged structural components, it is difficult to use the more advanced techniques of autoclave or resin transfer molding. The composites consisted of two sheets of interwoven carbon fiber pre-mold. A two-part resin epoxy consisting of PH2032 epoxy and PH3660 hardener is used with a weight ratio of 4:1. A total time of 24 hours at room temperature was used for final cure. The final microstructure of the composite is shown in Fig. 3. The Scanning Electron Microscopy analysis of the microstructure shows that the fibers are distributed in the matrix at random with a volume fraction of 10%, Fig. 3.

The tensile samples were constructed based on the ASTM (American Society of Testing and Materials) Standard Test Method D3039 (31). The tab materials were machined from a G-10 strip. Tensile tests of the carbon fiber/thixotropic composites were conducted before the creep and load relaxation. Initially, tensile tests were performed to produce stress strain curves at room temperature. Tensile tests were performed at 25, 40 and 60°C for a minimum of four specimens at each temperature conditions. An MTS machine equipped with an environmental chamber purchased from ATS was used to conduct the tensile tests. Each specimen was loaded at a constant crosshead rate of 0.15 mm/min until failure. The MTS machine was also used for the creep and relaxation tests. Creep tests were performed on the same MTS load frame. Two Micromeritics CEA-06-500UW-120 strain gauges were bonded on the center of the specimen, one on each face, to measure the longitudinal creep strain. A constant stress was achieved using TestStar™ closed-loop controller. The strain signal from the

Table 2. Typical properties of Thixotropic Epoxy.

Component	PH2032 Epoxy resin base	PH3660 Curing agent
Viscosity	90 N.s/m ²	95 N.s/m ²
Mix ratio by volume	3.2	1
by weight	100	27
Density	1.109 Kg/L	11.34 Kg/L
Glass transition temperature (T _g)	91.11°C	
Pot life (4 oz.)	—	50–60 min.
Tensile Strength (for 10 ply Laminate, 55% Glass fiber)	311 MPa	
Tensile modulus (for 10 ply Laminate, 55% Glass fiber)	17.6 GPa	

strain indicator was recorded by a data acquisition system. Each specimen was tested for one hour under 25, 40 and 60°C temperature environments, and the applied stress was set to the values of 50%, 70% and 90% of the corresponding strength under each temperature condition.

Standard tensile specimens were loaded for stress relaxation using the same load frame. Each sample was loaded at a constant displacement rate of 0.15 mm/min until a desired strain was achieved. At this point, a constant strain was maintained in the specimen. By maintaining a constant strain in the specimen, concern about the machine compliance was eliminated. The reduction of nominal stress with time was then measured for 1 hour per sample, using the

data acquisition system. The nominal stress/time history was then monitored and recorded for 1 hour. The relaxation tests were conducted under the same temperature conditions as before.

5. RESULTS AND DISCUSSION

The strength and elastic properties of the composite samples were measured from the stress-strain data at three different temperatures. Load as measured by the load cell was converted to stress using the average cross sectional area of the specimen measured prior to the test. Axial strain was calculated by averaging the readings of the two strain gauges. Five tests at each temperature were performed to obtain an average value for these properties, Table 3.

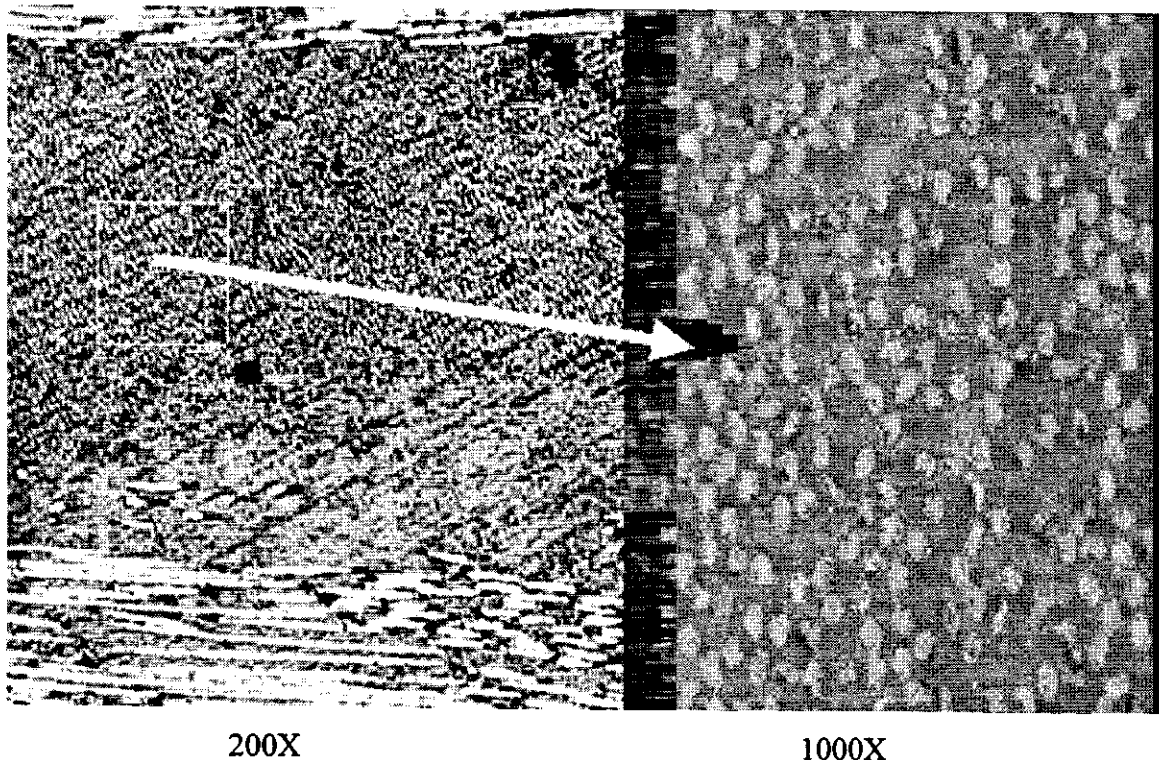


Fig. 3. The microstructure of the Thornel carbon fiber/Thixotropic epoxy matrix-using ESEM. The over all volume fraction was found to be 10%.

Table 3. Mechanical Properties at Three Temperatures Level.

T (°C)	σ_u (MPa)	E (GPa)
25	190.3 \pm 3.0	31.02 \pm 0.6
40	150.6 \pm 3.0	17.93 \pm 0.6
60	97.2 \pm 3.0	11.03 \pm 0.6

Tensile Tests Results

The effect of the temperature on the stress-strain behavior of the composite is plotted in Fig. 4. It is clear from the data that the elastic moduli and the strength decrease as the temperature increases. Since the 60°C is close to the glass transition temperature of the polymer matrix ($T_g = 91^\circ\text{C}$), the elastic modulus and strength have been decreased significantly to values 30% and 50 %, respectively, of those at room temperature. Table 1 shows the degradation of the strength and the modulus as the temperature increases. The values in Table 1 are the average values for 5 tests at each temperature.

Creep Tests Results

The experimental data from creep tests are plotted in Figs. 5–7, where the creep deformation was performed at three different stress levels for each temperature value. It was observed that at a temperature of 60°C, the sample failed to sustain the creep stress of 90% of the strength; this was observed for 3 different

samples under the same conditions to ensure the repeatability of this observation. It is noticed that with the application of load, an instantaneous strain response is developed, followed by a transient strain. A steady state (constant strain rate) creep develops during the strain history at larger time. A plot of the creep strain rate as a function of the holding stress is shown in Fig. 8. Significant creep strain rates were noticed, especially at higher stress levels. The strain rate range under different temperature and loading conditions was $4.3 \times 10^{-8} - 3.1 \times 10^{-7}$ (sec^{-1}). The stresses were normalized with respect to the ultimate tensile strength at the corresponding temperatures. A higher creep strain was noticed when the test specimen was held under a higher temperature. The modulus of the thermoplastic composite decreased at elevated temperatures; thus, that may have accelerated the creep response.

Load Relaxation Tests Results

Representative stress-time relaxation curves (stress-time) for the composite under different temperature conditions are presented in Figs. 9–11. The loading portion of each curve provides a measure of the elastic constant of the testing machine, K_m , as illustrated in Eq 3. The remainder of the curve is the relaxation history at fixed crosshead position of the testing machine. The final strain history is plotted as $\log(\sigma) - \log(\epsilon)$ curves as shown in the following. The analysis requires the use of apparent elastic modulus during the

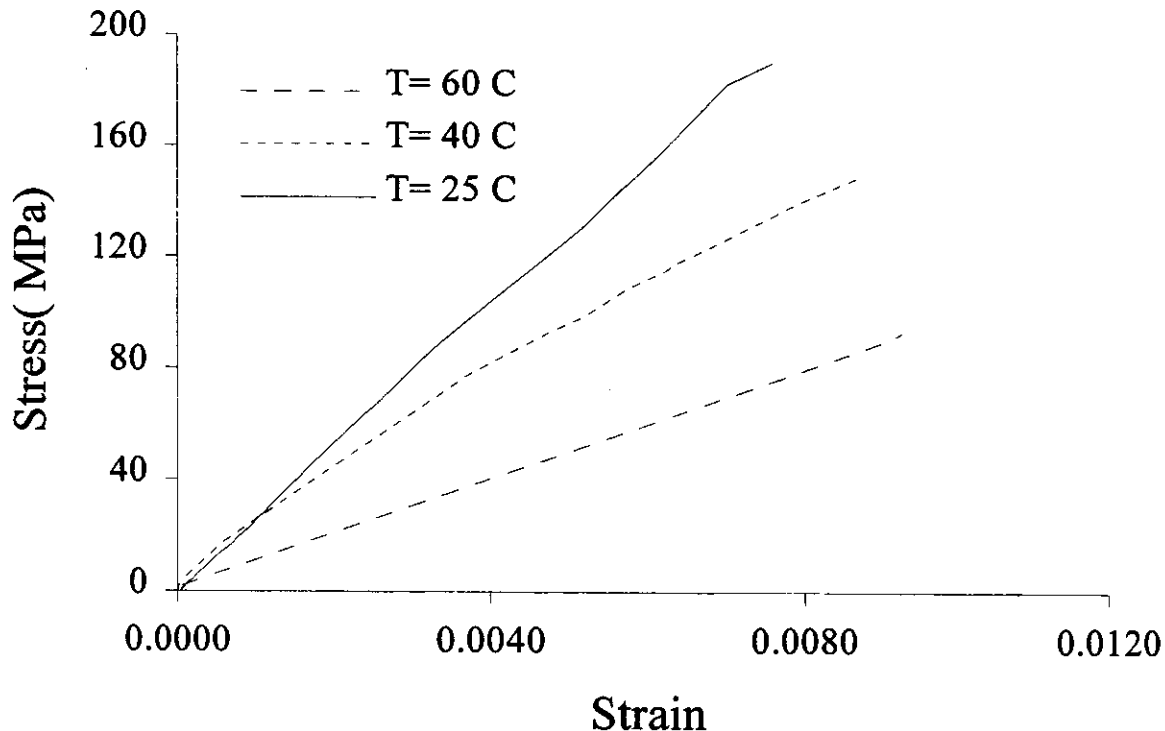


Fig. 4. Stress-strain curves for the tensile tests under different temperature environments.

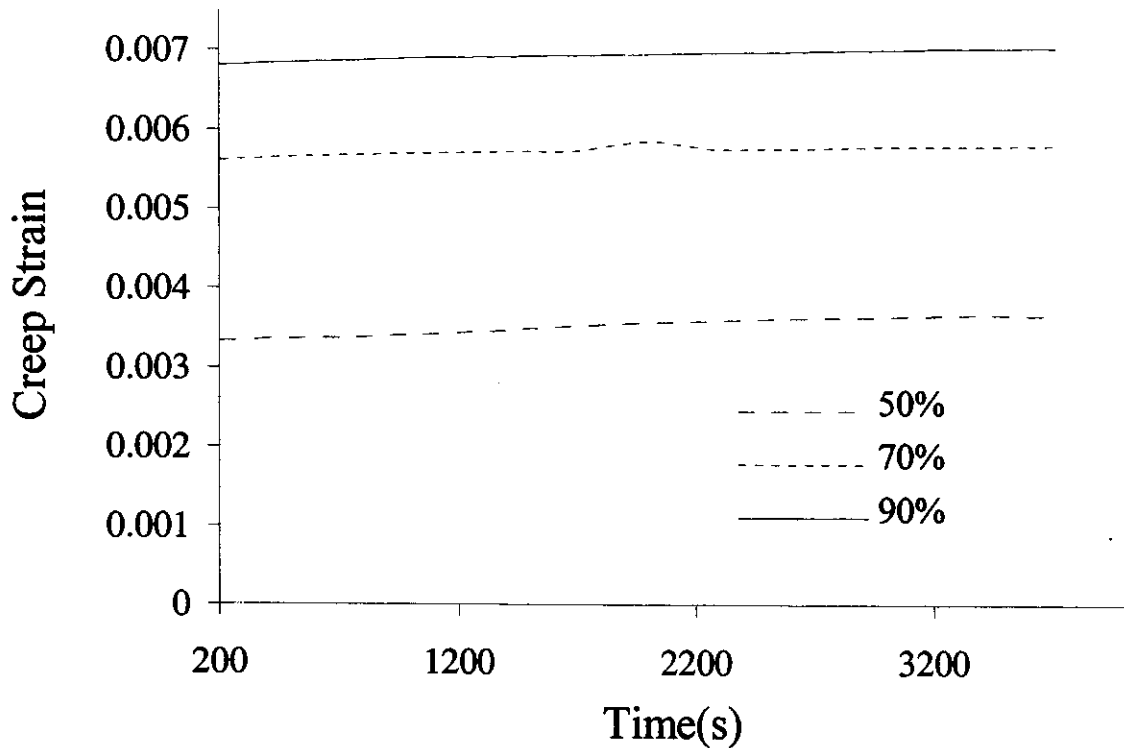


Fig. 5. Creep response of the composite at 25°C. The experiment was repeated for three different percentage of the yield strength.

uniaxial loading of the specimen. It was assumed that the total strain rate can be decomposed into an elastic ($\dot{\epsilon}_e$) and inelastic ($\dot{\epsilon}_i$) components;

$$\dot{\epsilon} = \dot{\epsilon}_e + \dot{\epsilon}_i \quad (16)$$

The elastic component of the strain is related to the applied stress by

$$\dot{\epsilon}_e = \frac{\dot{\sigma}}{E} \quad (17)$$

The total strain rate is zero ($\dot{\epsilon} = 0$) during the relaxation experiment, hence Eq 16 is reduced to

$$\dot{\epsilon}_e = -\dot{\epsilon}_i \quad (18)$$

and as a result the inelastic strain rate can be calculated from

$$\dot{\epsilon}_i = -\frac{\dot{\sigma}}{E_A} \quad (19)$$

where E_A is the apparent modulus given by Eq 7.

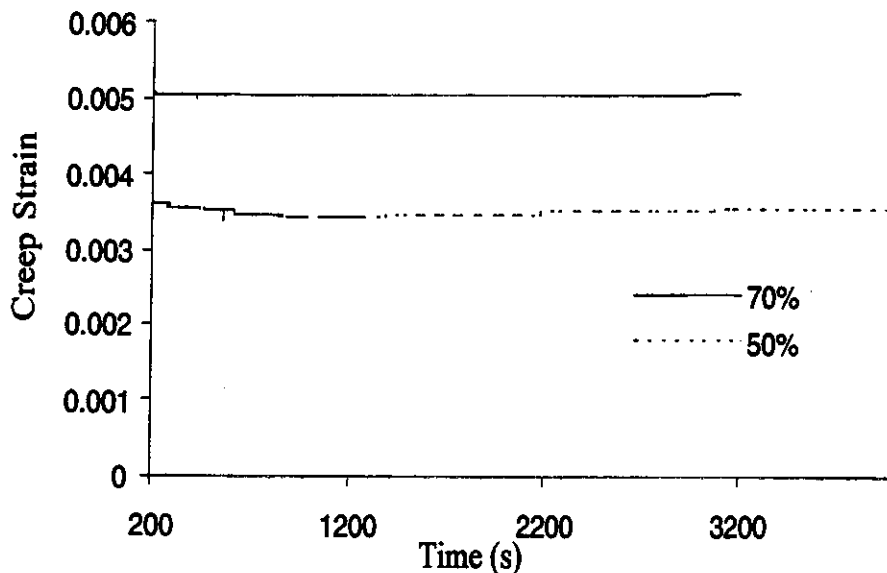
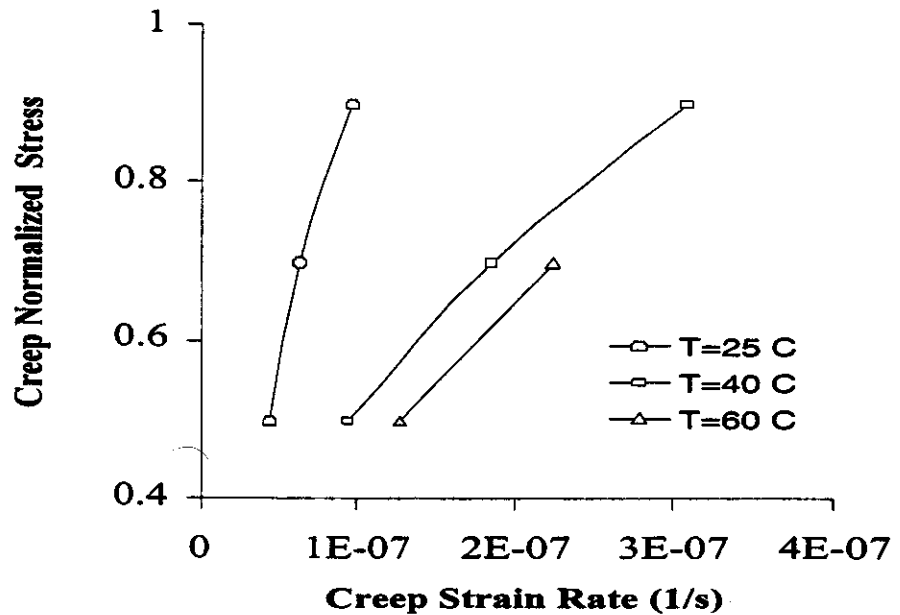


Fig. 6. Creep response of the composite at 40°C. The experiment was repeated for two different percentage of the yield strength.

Fig. 7. Creep response of the composite at 60°C. The experiment was repeated for two different percentage of the yield strength.



It is now clear that any sufficiently precise experimental record of the load and the time can yield a record of σ , ϵ , $\dot{\epsilon}$ as a function of time, where σ is the true stress, and $\dot{\epsilon}$ is the strain rate, and ϵ is the accumulated plastic strain.

To calculate the strain rate at any point in time, the time derivative of the stress is needed. The dependence of the stress on time is approximated by a best fit to a polynomial function of degree 10:

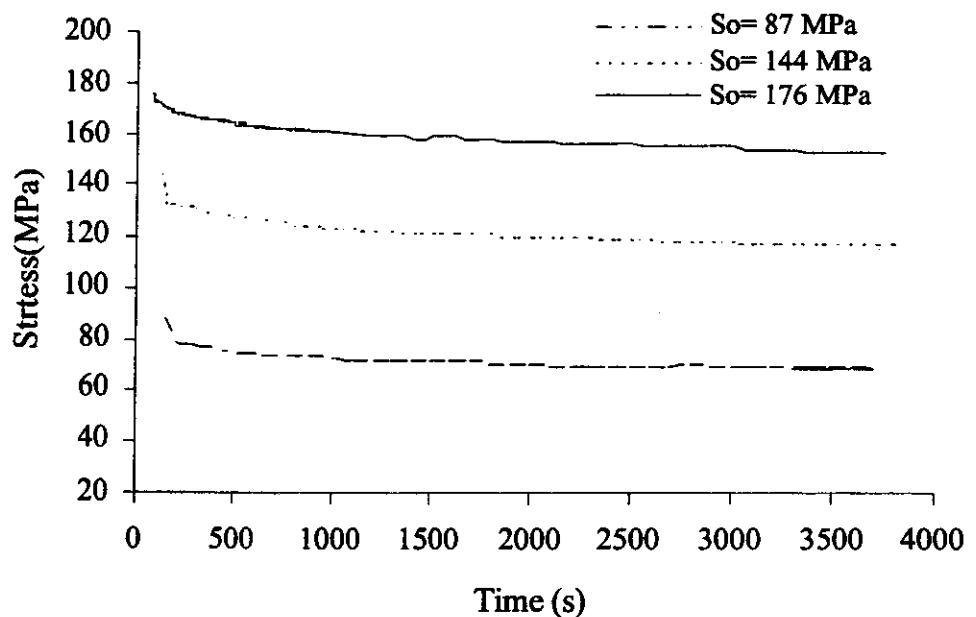
$$\sigma(t) = A_{10}t^{10} + A_9t^9 + \dots + A_0 \quad (20)$$

The proposed curve fitting for the load relaxation at 25°C and 90% of the strength is simulated in Fig. 12.

The curve fitting shows a satisfactory approximation to the original data. The Newton-Raphson algorithm was used to produce the curve fitting. There was no difficulty in differentiating the stress-time data over most of the stress history at higher strain rates. Somewhat poorer accuracy could be obtained at the very low strain rates end of the data. A similar conclusion was cited in Hart's work (25) by differentiating the stress with respect to time and using Eq 15.

The proper presentation of the relaxation result is the $\log(\sigma)$ - $\log(\dot{\epsilon})$ relationship. The main point to be made in this connection is that the load relaxation test is specially self-programmed sequence of stress

Fig. 8. Plot of the creep strain rate against the normalized stress. Normalization was performed against the corresponding tensile strength at each temperature.



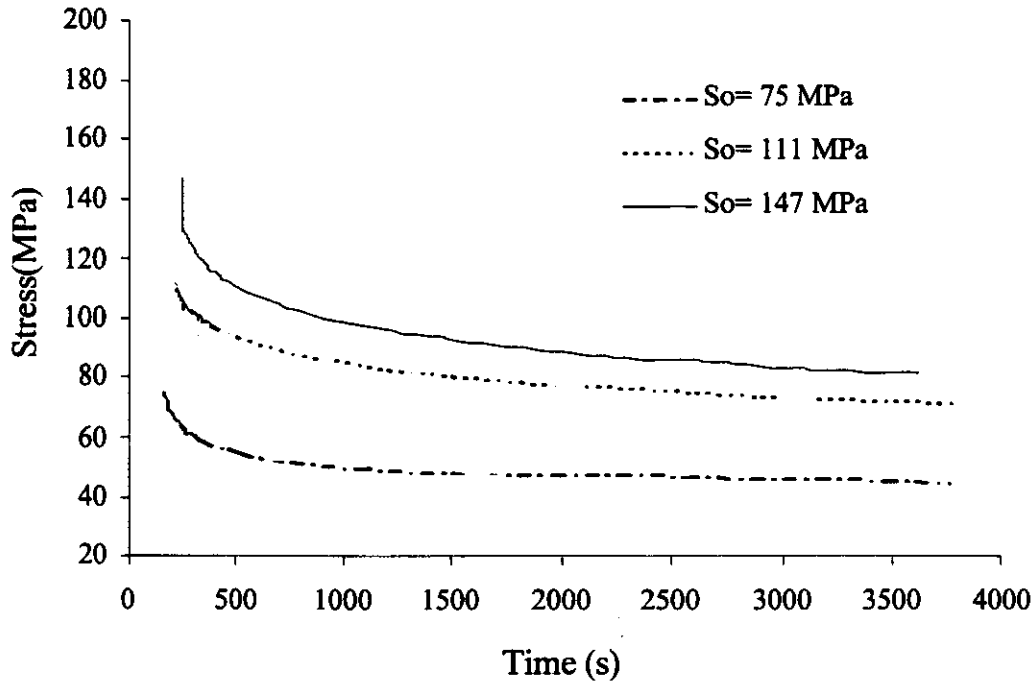


Fig. 9. Stress relaxation result at 25°C, the relaxation was initiated at different levels of stress

strain rate measurements carried out with very little plastic strain. It was observed that the rate of stress relaxation, as indicated by the slope, increases with the strain level. Of the three deformation variables, σ , ϵ , and $\dot{\epsilon}$, the two that are uniquely indicative of the mechanical state of the specimen are σ and ϵ . The large deformation of materials are usually associated with long-range structural changes. These can affect the hardness of the material as measured using a hardness test or the ultimate tensile strength as mea-

sured using a tensile test. Stress relaxation tests have been used to measure such a parameter for more uniform materials (polycrystalline metals at low and high temperatures) (25). This parameter is also related to the "Over-Stress" or threshold stress as is used in the models for the case of composites and more low temperature behavior of other materials. The stress - strain rate results are presented in Figs. 13-14. A detailed study of load relaxation tests to measure the hardness parameter for the two limiting cases of high

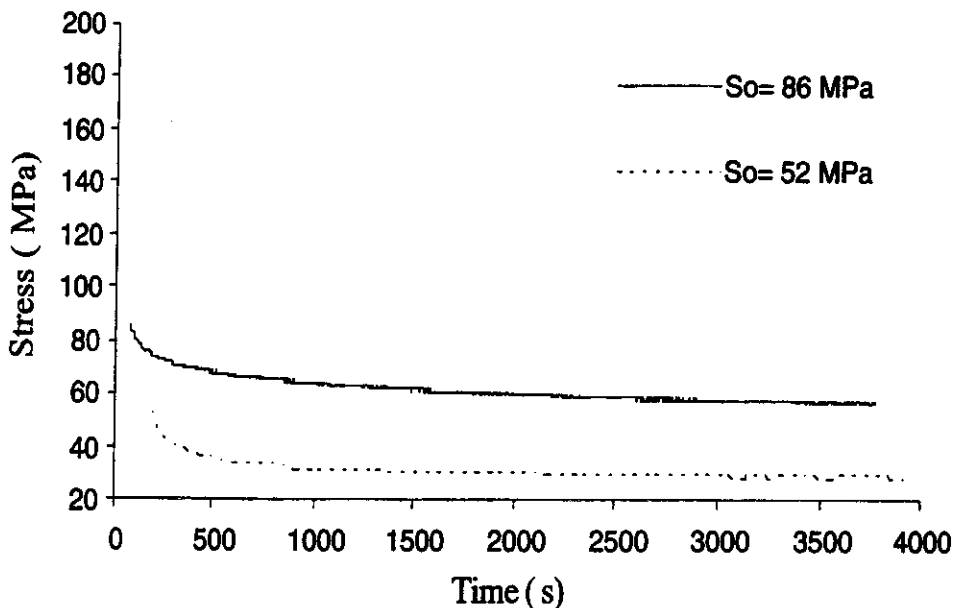


Fig. 10. Stress relaxation result at 40°C, the relaxation was initiated at different levels of stress.

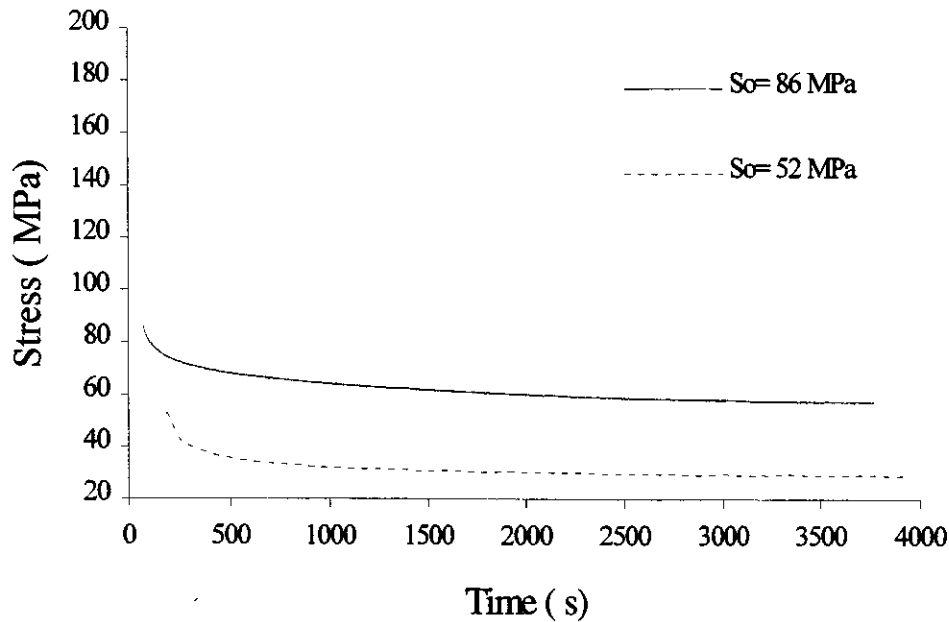


Fig. 11. Stress relaxation result at 60°C, the relaxation was initiated at different levels of stress.

and low temperatures was illustrated by Hart (25). The outstanding feature of all the $\log(\sigma) - \log(\dot{\epsilon})$ curves is the very large strain rate regime that is covered in each relaxation run. Also, the stress at the end of the relaxation test drops to a parameter usually referred to as *overstress*. Of particular importance in the viscoplastic analysis of composites, the overstress depicts the excess of the rate-dependent stress (from relaxation tests) over the stress at the same strain in tensile tests. The nature of $\log(\sigma) - \log(\dot{\epsilon})$ curves implies the existence of an overstress parameter because of the nonlinearity in the log-log scale horizontal slope at the

very low strain rates. If viscoplasticity (or inelasticity) is absent or if the behavior is completely plastic, the nonlinearity would be replaced by a horizontal line from the beginning of relaxation. Interestingly, for our materials the inelastic deformation was rate (time)-dependent even at room temperature. In Fig. 16, the relaxation stresses and their corresponding stress drops were normalized with respect to their respective ultimate tensile strength for each temperature. Both the temperature and the initial stresses are the control parameters, which control the time-dependent relaxation behavior of the composite.

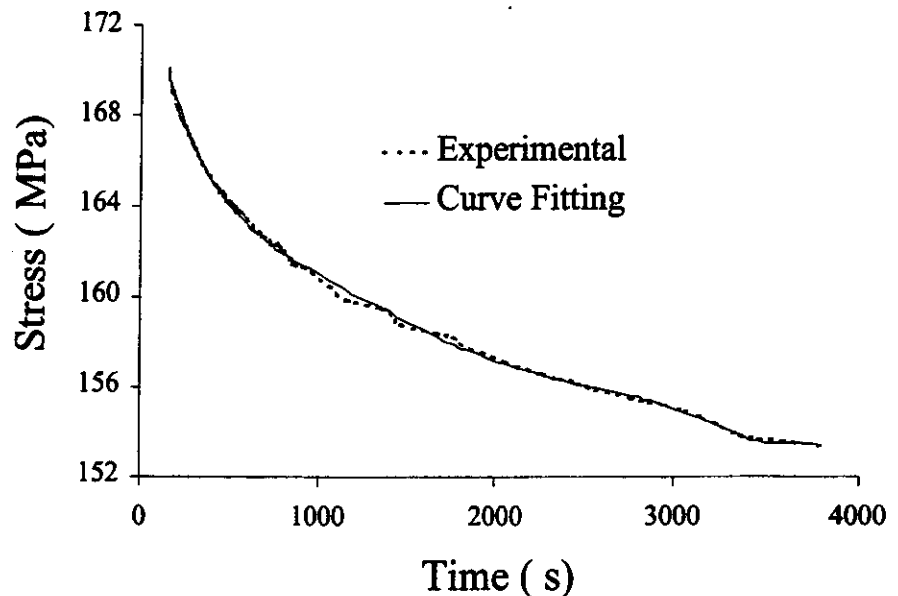


Fig. 12. Curve fitting for stress-time data at 25°C and 90% of the strength. The data were fitted into a polynomial of degree 10.

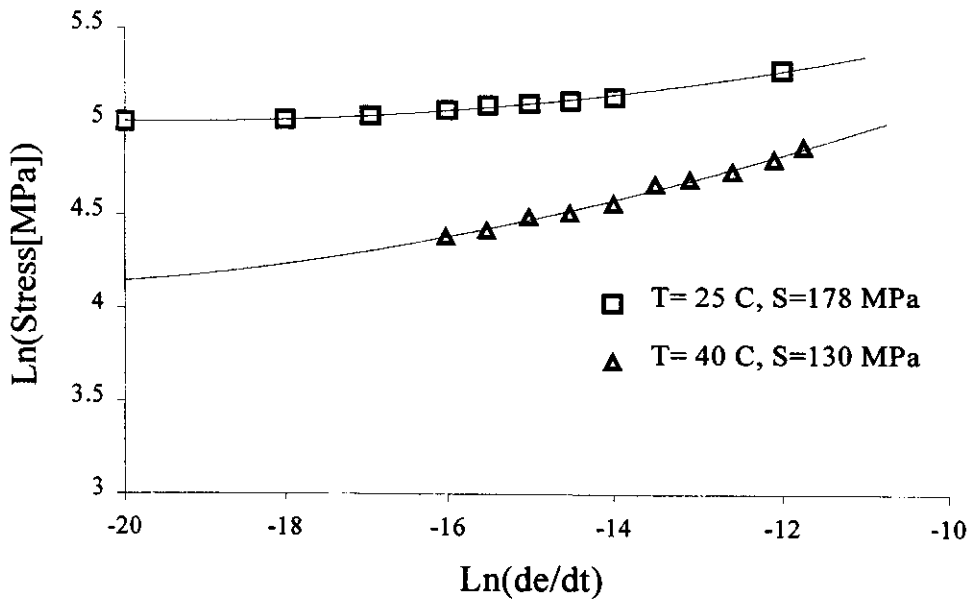


Fig. 13. Logarithmic plot of the stress and strain rate. The initial stresses were taken as 50% of the ultimate tensile strength at each temperature.

Interpretation of Creep and Load Relaxation Results

The wide range of strain rates covered in the $\log(\sigma)$ – $\log(\dot{\epsilon})$ curves makes the load relaxation test a more effective testing method than the long-time creep tests. This test is capable of predicting strain rates (usually obtained via creep tests) to several weeks from accelerated tests lasting a few hours. Usually the load relaxation is mistaken for a creep test. To clarify this, consider creep at 40°C at different levels of

stress. The strain rates can be deduced from the slope of the creep curves after a steady-state creep is reached. Thus, each creep experiment provides one single strain rate. On the other hand, a single load relaxation can produce a continuous distribution of strain rates for all stresses within a specific range. The stress range can be determined from the prior equations and depends upon the initial stress and time of relaxation. The results of the two approaches show that creep and relaxation experiments do not follow the same strain rate path, Fig. 17. There are

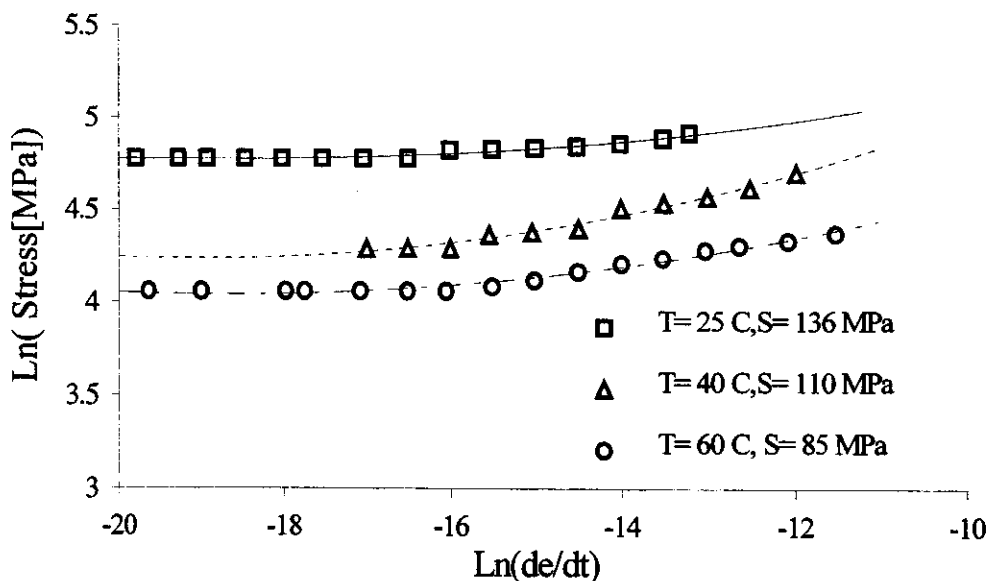


Fig. 14. Logarithmic plot of the stress and strain rate. The initial stresses were taken as 70% of the ultimate tensile strength at each temperature.

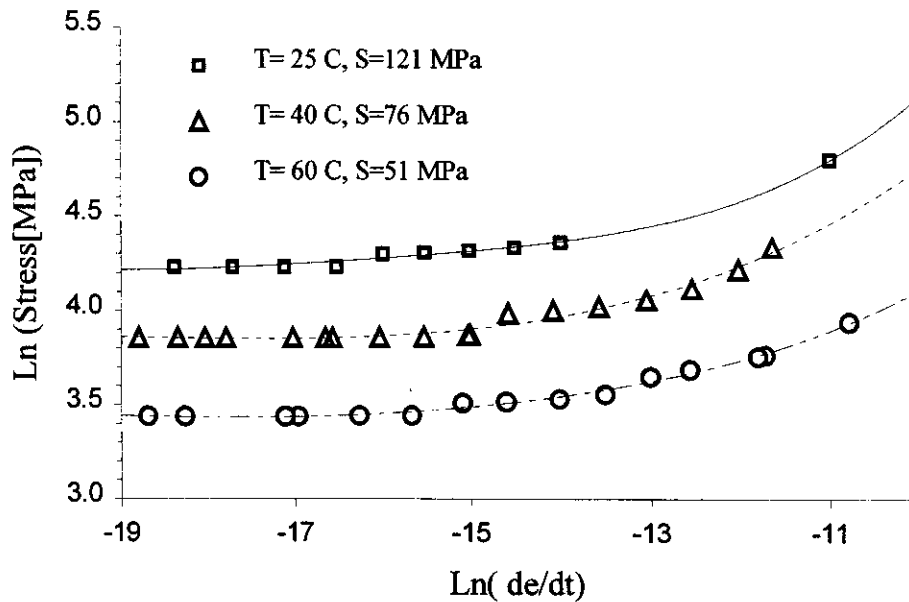


Fig. 15. Logarithmic plot of the stress and strain rate. The initial stresses were taken as 50% of the ultimate tensile strength at each temperature.

several reasons for this difference. First, creep requires a larger strain and as a result, it is accompanied with internal structural changes. Second, such structural changes may involve larger damage to the composite material (compared to relaxation test) and may involve other mechanisms such as fiber breakage and debonding.

6. CONCLUSIONS

The present work describes different short-time testing schemes to predict long-time viscoplastic behavior

of PMCs. The high temperature test results show that both the strength and elastic modulus degrade with an increase in temperature. The results show that the strength values drop significantly with temperature (from 190.3 MPa to 97.2 MPa at 60°C). Creep and stress relaxation tests measure the structure dimensional stability of the composite, and because the tests can be of long duration, such tests are of great practical importance. Creep of the composite has been investigated using the strain gauge method; the effect

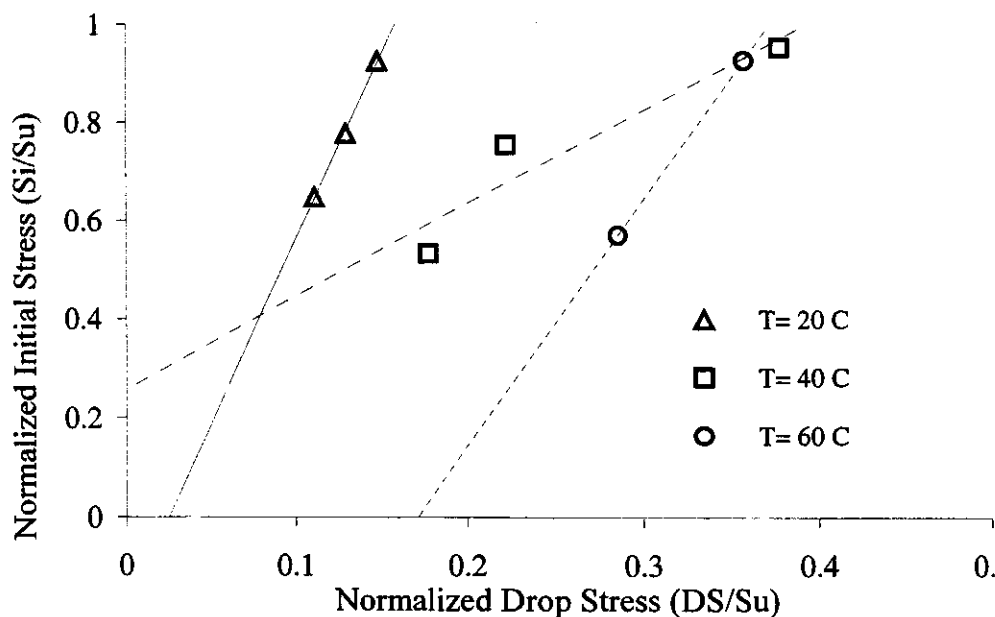


Fig. 16. Plot of the normalized initial stress level against the normalized stress drop. Normalization was taken w.r.t strength at the corresponding temperatures.

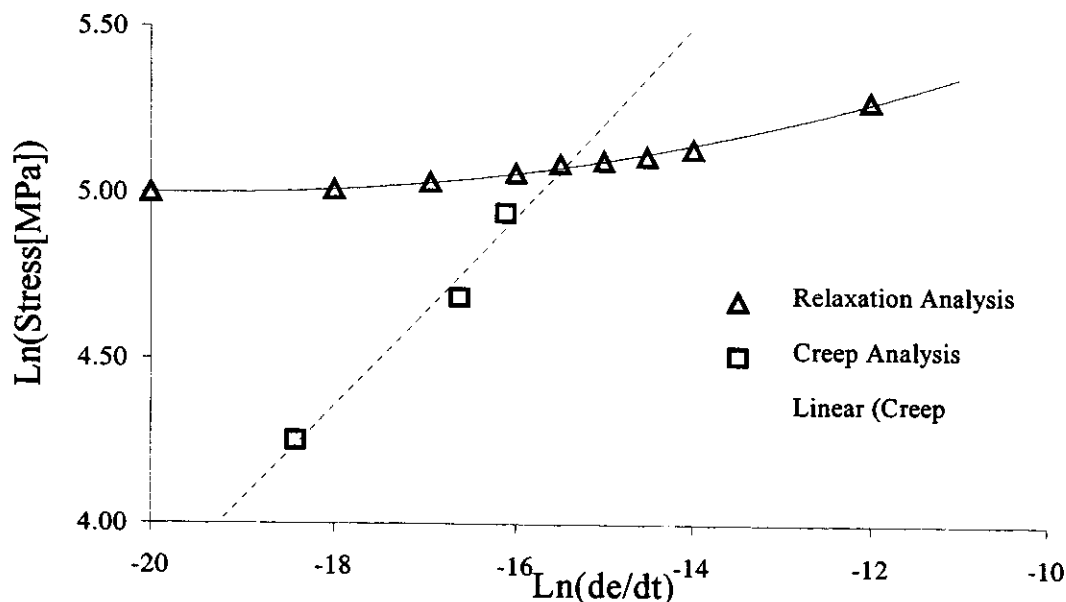


Fig. 17. Logarithmic plot of the stress and its corresponding strain rate as deduced from three creep tests and a single relaxation test at 25°C.

of holding stress, strain rate and temperature was established. Stress relaxation experiments have revealed the nature of the rate dependence deformation for long-term inelastic behavior. The relation between the load drop, temperature and strain level was investigated. Load relaxation methodology for generating long-term prediction of composite durability was proven to be more time and cost efficient than the traditional long-term tensile creep testing approaches.

ACKNOWLEDGMENT

The authors are grateful to the Structural Research Center, Florida Department of Transportation, for providing the materials used in this research.

REFERENCES

1. L. Franke and H. J. Meyer, *J. Mat. Sci.*, **27**, 4899 (1992).
2. R. J. Morgan, E. Shin, et al., *39th Intern. SAMPE Symp.*, 1564 (1994).
3. E. Shin, R. Dunn, and R. Morgan, *10th ASM/ESD Adv. Comp. Conf.*, 545 (1994).
4. M. J. Chajes, W. W. Finch, et al., *ACI Struct. J.*, **3**, 208 (1996).
5. S. J. DeTeresa, *JOM*, **8**, 58 (1993).
6. A. Pasricha, D. A. Dillard, and M. E Tuttle, *Comp. Sci. Tech.*, **57**, 1271 (1997).
7. D. R. Veazie and T. S. Gates, *AIAA*, **98**, 1 (1998).
8. T. S. Gates, *High Temperature and Environmental Effects on Polymeric Composites*, ASTM STP1174, 201 (1993).
9. T. S. Gates, *Composites Materials: Testing and Design*, 11th Volume, ASTM STP, 1206, 177 (1993).
10. A. Lee and G. B. McKenna, *Polym. Sci. B: Polym. Phys.*, **35**, 1167 (1997).
11. S. W. Case, R. B. Plunkett, and K. L. Reifsnider, *High Temperature and Environmental Effects on Polymeric Composites*, 2nd Volume, ASTM STP, **35** (1997).
12. E. E. Shin, R. Jurek, L. T. Drazel, and R. J. Morgan, *Proc. ASME Mat. Div.*, **163** (1995).
13. Y. Leterrier, Y. Wyser, and J. E. Manson, *J. App. Polym. Sci.*, **73**, 1427 (1999).
14. S. Zhu, S. Mizuno, et al., *Mat. Sci. and Eng.*, **A225**, 69 (1997).
15. H. L. McManus and R. A. Cunningham, *High Temperature and Environmental Effects on Polymeric Composites*, 2nd Volume, ASTM STP, **1** (1997).
16. T. S. Gates, *AIAA*, **2**, 925 (1999).
17. A. D. Drozdov, *Polymer*, **39**, 1327 (1998).
18. S. G. Baradenhagen, M. G. Stout, and G. T. Gray, *Mech. of Mat.*, **25**, 235 (1997).
19. J. Fish and K. Shek, *Comp Part B*, **29**, 613 (1998).
20. M. Vujosevic and D. Krajcinovic, *Int. J. Solids Structures*, **34**, 1105 (1997).
21. J. H. Shyr, E. A. Elsayed, and J. T. Luxhoj, *Naval Research Logistics*, **46**, 303 (1999).
22. J. Raghavan and M. Meshii, *Comp. Sci. and Tech.*, **57**, 1673 (1997).
23. J. Raghavan and M. Meshii, *Comp. Sci. and Tech.*, **57**, 375 (1997).
24. M. A. Meyers and K. K. Chawla, *Mechanical Metallurgy: Principles and Applications*, Prentice-Hall, Inc., Englewood Cliffs, N.J. (1984).
25. E. W. Hart and H. D. Solomon, *Acta Metallurgica*, **21**, 295 (1973).
26. E. W. Hart and H. Garmestani, *J. Exp. Mech.*, **3**, 1 (1993).
27. F. Booseshaghi and H. Garmestani, *Scripta Materialia*, **40**, 1359 (1999).
28. J. Lemaitre and J. L. Chaboche, *Mechanics of Solid Materials*, Cambridge University Press, New York (1990).
29. G.G. Grzywnski and D. A. Woodford, *Polym. Eng. Sci.*, **35**, 1931 (1995).
30. W. N. Findley, J. S. Lai, and K. Onaran, *Creep and Relaxation of Nonlinear Viscoelastic Materials*, Dover Publications Inc., New York (1989).
31. J. E. Masters and M. A. Portanova, *Standard Test Methods for Textile Composites*, NASA Contractors Report 4751 (1996).